See also: **II / Crystallization:** Polymorphism. **III / Biological Systems: Ion Exchange Biologically Active Compounds and Xenobiotics: Magnetic Affinity; Supercritical Fluid Crystallization**.

Further Reading

Addadi L and Weiner S (1989) Stereochemical and structural relations between macromolecules and crystals. In: Mann S, Webb J and Williams RJP (eds) *Biomineralization*, pp. 133–156. Weinheim: VCH.

Aizenberg J, Black AJ and Whitesides GM (1999) Oriented growth of calcite controlled by self-assembled monolayers of functionalized alkanethiols supported on gold and silver. *Journal of the American Chemistry Society* 121: 4500–4509.

Briat J-F and Lobréaux S (1998) Iron storage and ferritin in plants. In: Sigel A and Sigel H (eds) *Metal Ions in Biological Systems*, vol. 35, pp. 563–584.

Chasteen ND (1998) Ferritin. Uptake, storage, and release of iron. In: Sigel A and Sigel H (eds) *Metal Ions in Biological Systems*, vol. 35, pp. 479–514.

de Leeuw NH and Parker CS (1998) Surface structure and morphology of calcium carbonate polymorphs calcite, aragonite, and vaterite: an atomistic approach. *Journal of Physical Chemistry B* 102: 2914–2922.

Douglas T and Young M (1998) Host–guest encapsulation of materials by assembled virus protein cages. *Nature* 393: 152–155.

Fendler JH (ed.) (1998) *Nanoparticles and Nanostructured Films: Preparation, Characterization and Applications*. Weinheim: VCH.

Gider S, Awschalom DD, Douglas T *et al.* (1995) Classical and quantum magnetic phenomena in natural and artificial ferritin proteins. *Science* 268: 77–80.

Harrison PM and Arosio P (1996) The ferritins: molecular properties, iron storage function and cellular regulation. *Biochimica et Biophysica Acta – Bioenergetics* 1275: 161–203.

Harrison PM, Hempstead PC, Artymiuk PJ and Andrews SC (1998) Structure–function relationship in the ferritins. In: Sigel A and Sigel H (eds) *Metal Ions in Biological Systems*, vol. 35, pp. 435–477.

Heywood B (1996) Template-directed nucleation and growth of inorganic materials. In: Mann S (ed.) *Biomimetic Materials Chemistry*, pp. 143–173. Weinheim: VCH.

Jambor JL and Dutrizac JE (1998) Occurrence and constitution of natural and synthetic ferrihydrite, a widespread iron oxyhydroxide. *Chemical Reviews* 98: 2549–2585.

Lippmann F (1973) *Sedimentary Carbonate Minerals. Minerals, Rocks and Inorganic Materials*, vol. 6. Berlin: Springer-Verlag.

Lowenstam HA and Weiner S (1989) *On Biomineralization* (Eds Mann, Webb and R.J.P. Williams) New York: Oxford University Press, 7–49.

Möller M and Spatz JP (1997) Mineralization of nanoparticles in block copolymer micelles. *Current Opinion in Colloid and Interface Science* 2: 177–187.

Powell AK (1998) Ferritin. Its mineralization. In: Sigel A and Sigel H (eds) *Metal Ions in Biological Systems*, vol. 35, pp. 515–561.

Schäffer TE, Ionescu-Zanetti C, Proksch R *et al.* (1997) Does abalone nacre form by heteroepitaxial nucleation or by growth through mineral bridges? *Chemistry of Materials* 9: 1731–1740.

Simkiss K and Wilbur KM (1989) Molluscs – Epithelial control of matrix and minerals. In: *Biomineralization. Cell Biology and Mineral Deposition*, pp. 230–260. San Diego: Academic Press.

Weiner S and Addadi L (1997) Design strategies in mineralized biological materials. *Journal of Materials Chemistry* 7: 689–702.

DropBooks

Control of Crystallizers and Dynamic Behaviour

H. J. M. Kramer, Delft University of Technology, Delft, The Netherlands

Copyright © 2000 Academic Press

Introduction

Ideally industrial crystallizers are operated in such a way that the product specifications are met under conditions that permit profitable, trouble-free production of the desired crystalline material. In industrial practice, however, many operational problems can be encountered that reduce the performance of the crystallizer. The most commonly encountered problems are listed here.

- Deposition of crystal solids on the crystallizer internals, often called scaling or fouling. This results in a reduction of the heat transfer in the heat exchanger or leads to plugging of the process lines and can even hamper the flow pattern and thus the mixing in the crystallizer.
- Alternate feed composition. The resulting changes in the level of supersaturation in the crystallizer can lead to nucleation bursts or depletion of secondary nuclei, having a severe effect on the dynamics of the process.
- Disturbances in the heat exchanger in the crystallizer. This leads to variation in the production yield and the crystal concentration, which in turn

affects the attrition and nucleation kinetics of the process.
- Inappropriate seeding procedures. In batch crystallization processes problems often occur when the amount or size distribution of the seeds crystals or the time of seeding is not optimal. This will result in a final crystal size distribution that is off specification.
- Temperature changes in the crystallizer. This can result in dissolution of the fine crystals in certain zones in the crystallizer, which can have a large impact on the crystallizer dynamics.
- Water injection due to rinse procedures after blockage in product, recycle or circulation lines. This can also result in a temporary decrease in the supersaturation, causing internal dissolution of the fine crystals.

In addition slow, low-order oscillations of the crystal size distribution (CSD) are often observed, which are caused by internal feedback mechanisms in the crystallization process and periodically give rise to an excessive number of fine particles in the product.

To avoid these operational problems, all relevant process variables affecting the crystallization process must be kept within the acceptable limits defined during the design of the process. Not all of the process variables need to be controlled dynamically. Some of them are controlled directly by the equipment design, and others are directly coupled to other variables. Some must be actively controlled to enforce the right process conditions, for instance the temperature profile during a batch cooling process. Others must be manipulated to compensate for the effect of process disturbances. **Table 1** shows a list of the major process variables for continuous and batch processes. There has been extensive discussion in the literature about the role of each of the process variables and how they are controlled in a variety of crystallizer configurations.

Table 1 Process variables to be controlled in industrial crystallizers (after Rawlings *et al.*, 1995)

Continuous operation	*Batch operation*
Process temperature	(Rate of change in) process temperature
Heat flux to/from process	(Rate of change in) heat flux to/from process
Residence time of crystals	Batch time
Level (volume)	Level (FED batch)(volume)
Feed properties	
Concentration	
Temperature	
Flow rate	
Impurity level	
Slurry concentration	Slurry concentration
Purge flow	
Agitator and pump speed	Agitator and pump speed
CSD	CSD

The major process variables in a crystallization process are the level of supersaturation of the solvent, the energy dissipation, the CSD and the distribution of these variables over the crystallizer. These process variables determine to a large extent the kinetic processes (such as nucleation growth and agglomeration) that dominate the crystallization process. They interact with other process variables in a complex way. The presence of interactions and internal feedback mechanisms in the crystallization process limits the success of simple feedback control schemes and favours the use of model-based multivariable controllers, which are able to anticipate these interactions. Unfortunately multivariable control studies for industrial crystallizer are rare and almost completely lack experimental verification.

Depending on the type and scale of the crystallizers, the contents will not be uniformly distributed. Profiles are normally present in the temperature, concentration and particle concentrations, especially around heat exchangers and in baffle and boiling zones. It has recently been shown that the presence of such profiles can have a strong impact on the crystallizer performance. In general these inhomogenities are acceptable as long as the process variables within these zones stay within the acceptable limits and are time-invariant. The main problem in this respect, however, is that the process models normally used for control design do not take account of the presence of these profiles. Compartmental modelling, which has been used to improve the design of industrial crystallizers, should also be applied to control design.

This article gives an overview of the new developments in the control of the CSD for both continuous and batch crystallizers. Attention is focused on the direct control of the CSD either by simple, single-input/single-output feedback control or by multivariable control, using techniques that have been experimentally verified. The reason for this limitation is that process models normally used in crystallization research have a bad reputation with respect to their prediction of the process behaviour. Different crystallizer configurations are analysed with respect to available process actuators. In addition the process models, which form the basis for the controller design and the choice of the measurement technique, are discussed. Some excellent review articles on this topic are used as the starting point of this overview.

Modelling of Industrial Crystallizers

The development of an advanced control strategy requires a dynamic model that accurately describes the behaviour of the process. The derivation of such a model implies identification of the model structure and estimation of the model parameters using experimental data, and verification of the model. Parameter estimation falls beyond the scope of this article and will not be covered here.

The modelling of industrial crystallizers is dominated by the presence of the so-called population balance, which describes the evolution in time of the CSD in the crystallizer. The population balance provides a generally accepted approach to the modelling of dispersed phase systems and allows specification of the product quality in terms of the CSD. The general form of the population balance equation (PBE) is as shown in eqn [1]:

$$\frac{\partial(n(L)V)}{\partial t} = -V\frac{\partial(G_L(L)n(L))}{\partial L} + B(L)V - D(L)V + \sum_{j=1}^{m}\phi_{v,\text{in},j}\,n_{\text{in},j}(L) - \sum_{k=1}^{n}\phi_{v,\text{out},k}h_{\text{out},k}(L)n(L) \quad [1]$$

where the amount and the size of the crystals (or particles) are expressed in terms of number density $n(L)$ and crystal length L. V is the suspension volume in the crystallizer, with m streams entering and n streams leaving the crystallizer at volumetric flow rates of ϕ_v. $G_L(L)$ is the linear size-dependent growth rate, and $B(L)$ and $D(L)$ are birth and death rates respectively. Birth and death events can be caused by agglomeration and by the birth of small crystals, called nuclei. The classification function $h(L)$ describes the relation between the CSD in the crystallizer and that in an outlet stream.

As the PBE is a partial differential equation with respect to time t and crystal length L, two boundary conditions are needed to solve it analytically:

$$n(0,t) = \frac{B_0}{G_L(0)} \quad [2]$$

$$n(L,0) = \text{initial distribution} \quad [3]$$

As primary and secondary nucleation typically involves the birth of small crystals, nucleation is often presented as the birth of nuclei at zero size. Instead of a birth term in the PBE for the nucleation event $B(L)$ that happens over a size range $0 \le L \le y$, the birth rate B_0 given by boundary eqn [2] is used. These two are related as shown in eqn [4]:

$$B_0 = \int_0^y B(L)\,dL \quad [4]$$

For the second boundary condition a seed population or a population formed by the outgrowth of primary nuclei can be substituted.

The mass balance is given by eqn [5]:

$$\frac{dM_{\text{total}}}{dt} = \phi_{v,\text{feed}}(\varepsilon_{\text{feed}}\rho_{\text{feed,liquid}} + (1-\varepsilon_{\text{feed}})\rho_{\text{crystal}}) - \phi_{v,\text{product}}(\varepsilon\rho_{\text{liquid}} + (1-\varepsilon)\rho_{\text{crystal}}) - \phi_{v,\text{vapour}}\rho_{\text{vapour}} \quad [5]$$

The component balances are given by:

$$\frac{dM_i}{dt} = \phi_{v,\text{feed}}(\varepsilon_{\text{feed}}\rho_{\text{feed,liquid}}w_{\text{feed,liquid},i} + (1-\varepsilon_{\text{feed}})\rho_{\text{crystal}}w_{\text{feed,crystal},i}) - \phi_{v,\text{product}}(\varepsilon\rho_{\text{liquid}}w_{\text{liquid},i} + (1-\varepsilon)\rho_{\text{crystal}}w_{\text{crystal},i}) \quad [6]$$

where $i = 1, \ldots, N_{\text{comp}}$, and:

$$M_i = V(\varepsilon\rho_{\text{liquid}}w_{\text{liquid},i} + (1-\varepsilon)\rho_{\text{crystal}}w_{\text{crystal},i}) \quad [7]$$

where component $i = 1$ is the main compound to be crystallized, and components $i = 2, 3, \ldots, N_{\text{comp}}$ are the impurities present.

The distribution coefficients relate the impurity uptake by the solid and the concentration of the impurity in the liquid phase, as shown in eqn [8]

$$k_{\text{distr.},i} = \frac{w_{\text{crystal},i}}{w_{\text{liquid},i}} \quad [8]$$

where $i = 2, \ldots, N_{\text{comp}}$.

The enthalpy balance with the production rate or solids production P is given by eqn [9]:

$$\frac{dH}{dt} = \phi_{H,\text{feed}} - \phi_{H,\text{product}} - \phi_{H,\text{vapour}} + Q_{\text{heat}} + P\Delta H_{\text{cr}} \quad [9]$$

in which H denotes the enthalpy of the crystallizer content and ϕ_H the enthalpy of the particular stream. Q_{heat} is the effective heat input to the system including heat losses.

In order to complete the model, relations are needed for nucleation and growth. In many cases a size-independent growth rate is determined with a power law relation, as shown in eqn [10]:

$$G_L = k_g\sigma^g \quad [10]$$

DropBooks

where σ is the relative supersaturation. For the secondary nucleation a comparable function is used (eqn [11])

$$B_0 = k_N \sigma^b N^b M_T^j \qquad [11]$$

in which N is the stirrer frequency and M_T is the total crystal mass in the crystallizer. Note that B_0 and not B is calculated with this relation. Although these functions are still used, especially in controller design studies, it has been shown that in reality the growth rate function is more complicated and size dependent. In addition, the power law for the nucleation given in eqn [11] is not suitable for describing the dynamics in secondary nucleation dominated crystallization systems and improved relations have proven to give a much better description of these kinetic processes. Here the relations are used because they have been applied in controller design studies. The growth rate is given by eqn [12]:

$$G_L(L) = \mathrm{p6}(C - C_s)^{\mathrm{p7}}\left(1 - \frac{L^{\mathrm{p8}}(L_e^{\mathrm{p8}} + L^{\mathrm{p8}})}{L_e^{\mathrm{p8}}(L^{\mathrm{p8}} + L_a^{\mathrm{p8}})}\right) \qquad [12]$$

in which L is the crystal size. In this relation the growth rate decreases beyond a certain crystal size L_a due to attrition, while L_e is the maximum crystal size of the crystals. p6, p7 and p8 are model parameters, which have to be estimated. The relation for the secondary nucleation is shown in eqn [13]:

$$B_0 = \mathrm{p3}\left[\int_{\mathrm{p4}}^{\infty} n(L,t) L^{\mathrm{p5}}\, \mathrm{d}L\right]^{\mathrm{p1}} (C - C_s)^{\mathrm{p3}} \qquad [13]$$

Here B_0 is calculated assuming that the nuclei have a negligible size. Note that only crystals beyond a certain size p4 contribute to the secondary nucleation.

State Space Models

The design of model-based controllers requires a state space representation of the process model. As the population balance is a first-order nonlinear partial differential equation, a transformation must be used to get such a form.

Using the definitions of the moments of the distribution, the population balance can be transformed into a set of moment equations (eqn [14]):

$$m_j = \int_0^{\infty} n(L) L^j \, \mathrm{d}L \qquad [14]$$

For a continuously operated system with no impurities, a constant V, a size-independent growth rate, no agglomeration, nucleation at zero size, one crystal-free inlet stream, and a nonclassified product stream, the population balance (eqn [1]) simplifies into eqn [15]:

$$\frac{\partial n(L)}{\partial t} = -G_L \frac{\partial_n(L)}{\partial L} - \frac{n(L)}{\tau} \qquad [15]$$

with similar boundary conditions. This equation can be reduced to a set of ordinary differential equations using the moment transformation (eqn [16]):

$$\frac{\mathrm{d}m_j}{\mathrm{d}t} = jG_L m_{j-1} - \frac{m_j}{\tau} + B_0 L_0^j \qquad [16]$$

The first four moment equations, together with the kinetic relation (eqns [10] and [11]) and the mass, energy and component balances, form a closed set which describes the crystallization process. Unfortunately, the description will not be very realistic because of the large simplifications which form the basis of this description.

Other methods have been used to obtain a state space model. First of all the method of lines is applied to solve the population balance yielding a state space representation. For controller design this high order nonlinear model was first linearized and then further reduced. As an alternative a black box model was derived using system identification techniques.

Crystallizer Configurations

For continuous crystallization processes several types of crystallizer have been developed, which are used for different applications. The most common types of crystallizers are listed here.

- Forced circulation crystallizer (see **Figure 1**A). The most widely used crystallizer. It is often treated as a well mixed crystallizer, although several studies have shown that large variations in supersaturation exist within the crystallizer volume. Therefore crystal growth is limited to a small part of the crystallizer (in the vicinity of the boiling zone), and depending on the temperature rise in the external heat exchanger, even dissolution of the fine crystals will take place in that part of the crystallizer. Actuators to control the crystal size distribution are limited although configurations exist with an elutriation leg in which selective removal takes place. The level of supersaturation can be affected by control of the evaporation rate, while the profile can be influenced by adapting the circulation flow rate through the external heat exchanger. The main operational problems encountered with this type of crystallizer are scaling in the boiling zone or in the heat exchanger.

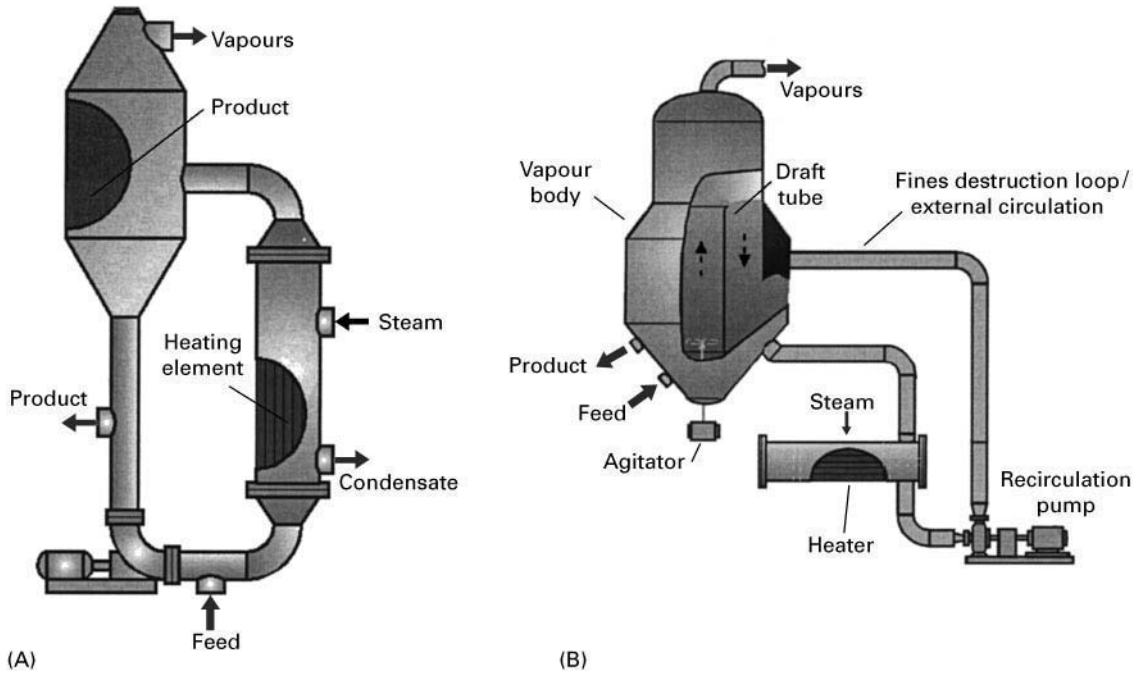

Figure 1 (A) Forced circulation and (B) stirred draft tube baffle (DTB) crystallizer with an external heat exchanger and fines destruction. Both crystallizers are produced by USFilter's HPD.

- Draft tube baffled (DTB) crystallizer (see Figure 1B). This crystallizer enables the generation of larger crystals using fines removal, which is done by installing a skirt baffle to create a settling or annular zone. The flow in the draft tube thus has to be upwards, which is effected by the impeller that also creates most of the attrition fragments. The fines flow can be diluted or heated to partly or totally dissolve the fines. An increase in the fines removal flow increases the number of fines that are removed from the crystallizer, but also increases the cut size of the fines. The fines loop in this way serves as an actuator that can be applied for control of the mean crystal size, although the variation in mean crystal size that can be achieved is limited. The elutriation leg, when present, serves more as a washing device to remove the impurities from the crystal than as a product classifier. The DTB crystallizer is among the best-studied crystallizers, because of the low order oscillations which are often observed. Other operational problems are scaling in the boiling and baffle zones.
- Fluidized-bed crystallizer (see **Figure 2**A). This crystallizer is especially designed to produce large and uniformly sized crystals. At the top of the bed the crystals are settled, and only the fines leave the crystallizer with the exhausted mother liquor to be circulated through the heat exchanger after mixing with the feed stream. The hot circulated flow enters the vaporizer head, where the solvent is flashed off. The supersaturated solution leaves the vaporizer through the downcomer, and enters the densely packed fluidized bed at the bottom of the crystallizer. The supersaturation is consumed on its way up, and a coarse product leaves the crystallizer at the bottom. The main control problems are stabilizing the fluidized bed and keeping the supersaturation in the circulation loop, and specifically in the boiling zone and the downcomer, within certain limits to prevent spontaneous (primary) nucleation. Also low-order cycling occurs in this type of crystallizer, which is however much less well studied than the DTB crystallizer. Although fines dissolution already takes place in the circulation loop, a separate fines removal loop can be installed to control the CSD in the crystallizer. In addition a clear liquor overflow stream is sometimes used to control the slurry density in the fluidizer (double draw off).
- Cooling crystallizer (see Figure 2B). In this crystallizer the slurry is circulated through a heat exchanger. For crystallization from solution the slurry is pumped through a tube and shell heat exchanger, with a ΔT range between the tube and the wall of 5–10°C. The temperature decrease in the heat exchanger must be controlled precisely.

As can be seen from these descriptions, the number of available process inputs to manipulate the CSD in the crystallizer is rather limited. The actuator most used

DropBooks

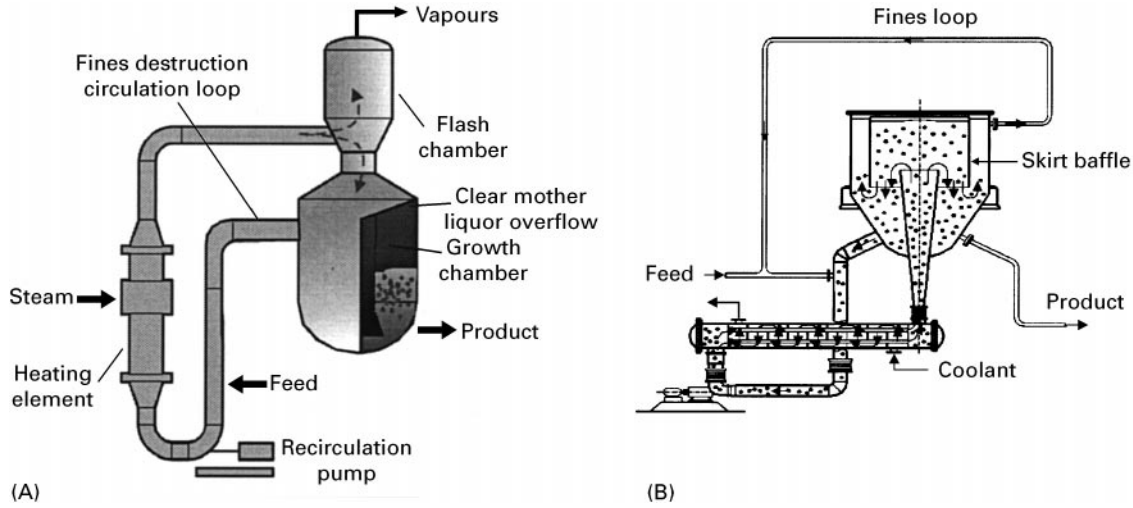

Figure 2 (A) Fluidized bed crystallizer from USFilter's HPD and (B) cooling crystallizers from Swenson.

in control studies is the fines dissolution flow rate, although in industrial crystallizers this flow cannot be manipulated freely. It is constrained on the lower side by the heat input of the system and by the maximum temperature increase of the fines flow. Selective product removal using an external product classifier such as a wet screen or a hydrocyclone seems to be an attractive additional process actuator method, which can be implemented irrespective of the crystallizer used.

Measurements

The on-line measurement of the relevant process variables forms an essential and often difficult part of the control strategy. For the CSD control the most relevant process variables are the supersaturation and one of the characteristics of the CSD. The main measurement techniques are summarized next.

- Supersaturation. Except for some crystallization systems (sugars) the direct measurement of supersaturation is either impossible or not accurate enough for control purposes. Recently however several studies have shown that it is possible to measure the supersaturation on-line in a crystallizer using attenuated total reflection (ATR) probes in combination with Fourier transform infrared (FTIR) devices. Successful applications of density measurements have also been reported.
- On-line CSD measurement. A number of commercial instruments are available nowadays to determine CSD of crystal slurries. Of these the laser diffraction instruments have been shown to give a reliable measurement in diluted suspensions (at particle concentrations below 1 vol%). A major drawback to the use of these instruments in a process is the need for an on-line dilution system to dilute the crystal suspension. A more recently developed instrument, measuring the attenuation of planar ultrasonic waves, forms an interesting alternative, because suspensions up to a concentration of 30% (by volume) can be measured without dilution.
- In-line CSD measurement. In-line sensors measuring the reflection of laser light and analysing the back-scatter peaks or images enable the analysis of some properties of the CSD inside the crystallizer, which can be of value for control of crystallizers. The main difficulty with the use of these probes is in identification of the relation between the information from the sensor and a process variable which is relevant for the control of the process.
- Obscuration measurement. The obscuration is defined as the fraction of light that is obscured by the crystals present in a flow cell and is a measure of the second moment of the distribution. As with laser diffraction this relation is only valid when multiple scattering can be avoided, i.e. at low particle concentrations. Obscuration measurements have been used to measure the number of fines crystals present in the fines removal loop.
- Particle counter. An optical particle counter measures the number of particles in a predefined size window in the crystallizer simply by counting the number of pulses from a light detector that are caused by the passage of the particles through a laser beam. The size window is defined as a result of the classification function of the funnel used to withdraw the process liquid from the crystallizer and the detection threshold of the detector, which can be adapted. This counter, which has been

successfully used to control a DTB crystallizer on a pilot-plant scale, forms an attractive alternative to the expensive CSD measurement devices.

The choice of the signal used by the controller, as well as the choice of the instrument, can be decisive for the performance of the controller. Using a CSD measurement, different characteristics of the CSD can be chosen. Analysis of different possibilities suggests that a reduced signal based on a principle component analysis of the raw diffraction data of a Malvern laser diffraction instrument, *y_r, gave the best controller behaviour*. The median crystal size, however, does not appear to be a suitable signal for control of the CSD, because of large delays in the response and its low sensivity for changes in the small crystal area.

Control of Continuous Crystallizers

Crystallization Dynamics

As indicated in the introduction, problems in the operation of continuous crystallization processes can lead to large disturbances in the dynamics of an industrial crystallizer. In addition, slow oscillations in the CSD may occur, which do not seem to be caused by process disturbances, but are an intrinsic property for certain process configurations and are related to the internal feedback mechanisms which are present in the crystallization process. This so-called slow cyclic behaviour is only seen in DTB and fluidized bed types of crystallizer configurations in the presence of fines dissolution and/or classified product removal. **Figure 3** shows an example of this behaviour for a 1000 L evaporative DTB crystallizer. For higher values of the fines removal flow rate a limit cycle was reached in the median crystal size, during which the median crystal size varied between 240 and 1040 μm in cycles of about 5–6 h. Oscillatory behaviour has also been reported after selective product removal.

The stability of an open loop continuous crystallizer has been the subject of many studies. The techniques used involve the Laplace transformation of the linearized version of the population balance or conversion to a set of ordinary differential equations using the moment transformation. These solution methods, however, pose severe limitations on the models.

Based on a stability analysis, two types of unstable behaviour, have been identified, namely low order and high order cycling. High order cycling can be caused by very high orders in the power law equation for the nucleation kinetics, which seems unlikely for most crystallization systems. Low order cycling on the other hand can be caused by nonrepresentative product removal.

In more recent work it has been established that simple power law kinetics are unable to explain the

DropBooks

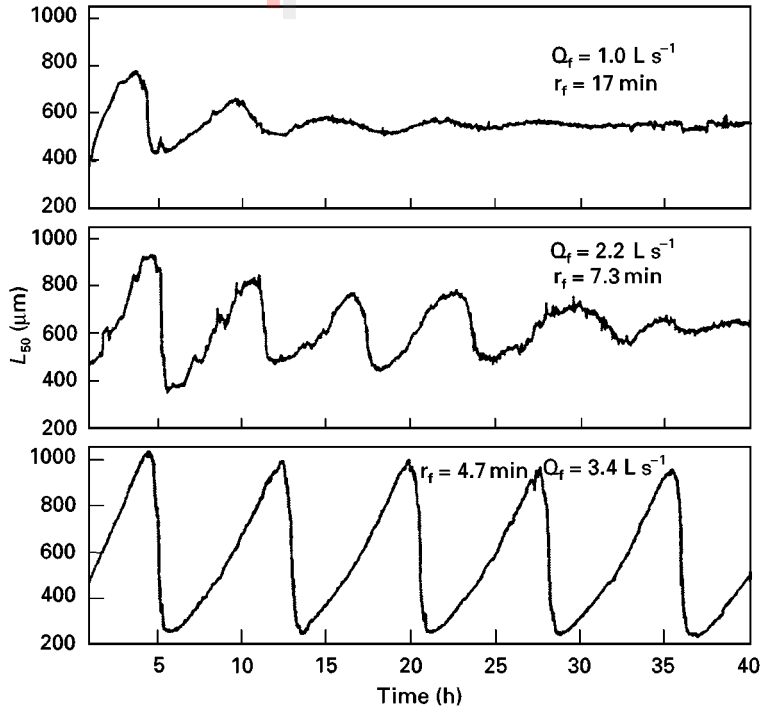

Figure 3 Experimental time response in a DTB crystallizer at start-up of the median crystal size for different fines removal flows (θ_f) and thus different residence times for the fines (r_f). *Eek et al.*, 1995b.

dynamic behaviour in industrial DTB crystallizers. Nucleation models that only take into account crystals beyond a certain minimum crystal size have been shown to give a much better description of the crystallization kinetics.

Some of these limitations in the stability analysis have been removed by using modern analytical techniques, which are based on the reduction of the system of balance and kinetic equations into one single integro-differential implicit equation. The steady state solution of this equation and that of the linearized equation around that point enables an analysis of more complex crystallization models.

Feedback Control

Experimental studies of feedback control schemes for laboratory and bench scale crystallizers have been based on the measurement of the suspension density in the fines removal line by manipulating the fines removal flow. The major drawback of this method is that the manipulation of the fines stream influences not only the number of crystals in the fines flow but also the cut-size of the baffle zone. Therefore the controller will in essence control the fines density removed from the system and not the fines density in the crystallizer.

An in-line Lasentec probe has been used to control a 1000 L DTB crystallizer producing potassium chloride using the fines removal flow as a process actuator. Problems identifying the optimal signal from the sensor and process disturbances affecting the CSD measurements decreased the efficiency of the controller.

The most complete study was one in which the fines removal rate was used as the process actuator to control the process. **Figure 4** shows the general control scheme in which u is the process input on which the controller acts, in this case the fines removal rate t and y the process output. d and m are possible process disturbances and the measurement noise respectively.

An on-line particle counter, measuring the number of crystals in a predefined size range (60–100 μm), was used. The control equation is then shown in eqn [17]:

$$Q_{\mathrm{f}} = k_{\mathrm{p}}\left(\varepsilon_n + \frac{T}{T_i}\sum_{n=0}^{k}\varepsilon_k\right) \qquad [17]$$

$$\varepsilon_n = N_{\mathrm{f}} - N_{\mathrm{f,setpoint}}$$

The error ε_k is the difference between the counter output and the set-point value. T is the sample time and T_i the integral or reset time. The following functions of the controller were tested.

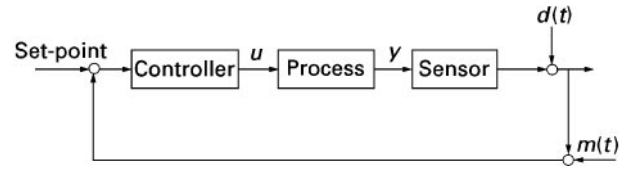

Figure 4 Feedback single-input/single-output control scheme.

1. Stabilization of the process. A considerable reduction in the oscillations after start-up was obtained in closed loop compared with the open loop behaviour (see **Figure 5**). The severe oscillations resulting from the onset of a product classifier (wet screen) could also be suppressed by the controller (see **Figure 6**)
2. Set-point tracking. The set-point in the number of fines could be followed by the controller. The changes in the set-point for the number of fines also resulted in changes in the median crystal size of the crystal produced.
3. Disturbance suppression. A process disturbance introduced in the process by closing the product flow for 1 h was analysed. It was shown that open loop response on the disturbance was almost completely suppressed in closed loop operation of the process (see **Figure 7**).

The choice of the size range for the particle counter, which could be affected by the detector threshold and the settling velocity in the funnel used to discharge the particles from the crystallizer, is essential for the performance of the controller. It has been shown that when the detection size range is moved to particles below 40 μm the controller becomes unstable.

As an alternative to the particle counter, the reduced signal of the laser diffraction instrument was used. Similar results were be obtained (see Figure 6).

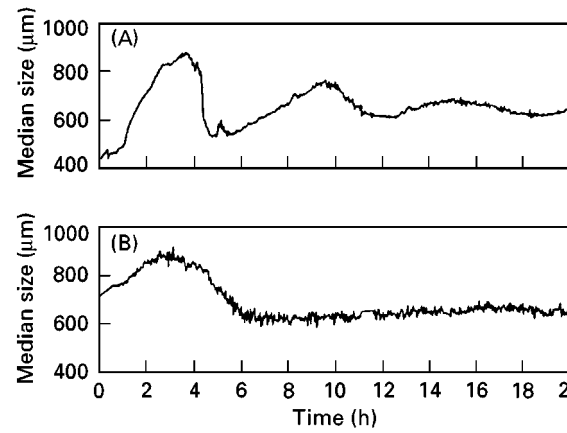

Figure 5 (A) Open and (B) closed loop start up trend of the median crystal size. (Eek, 1995)

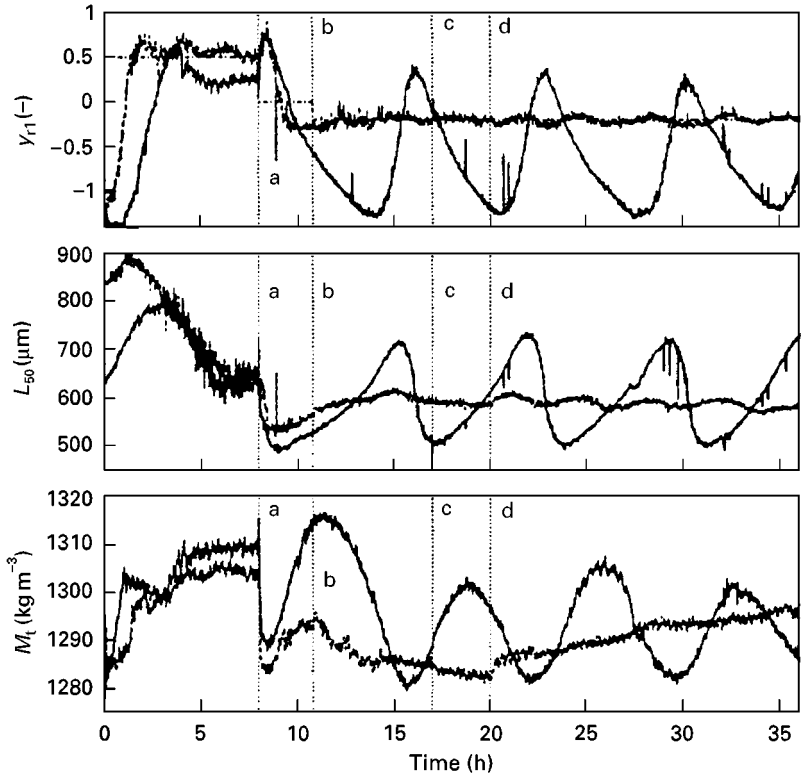

Figure 6 Open and closed loop trends in the y_r, the x_{50} and the total crystal mass after the onset of a product classifier at a. Points b, c and d represent changes in controller set point and product flow rate respectively. (Eek, 1995.)

DropBooks

Multivariable Control

Only a limited number of multivariable control studies is available and only one of them has been tested experimentally. A state space model must be the basis for a multivariable control design:

$$\dot{x} = A(t)x(t) + B(t)u(t)$$
$$y = C(t)x(t) + D(t)u(t) \qquad [18]$$

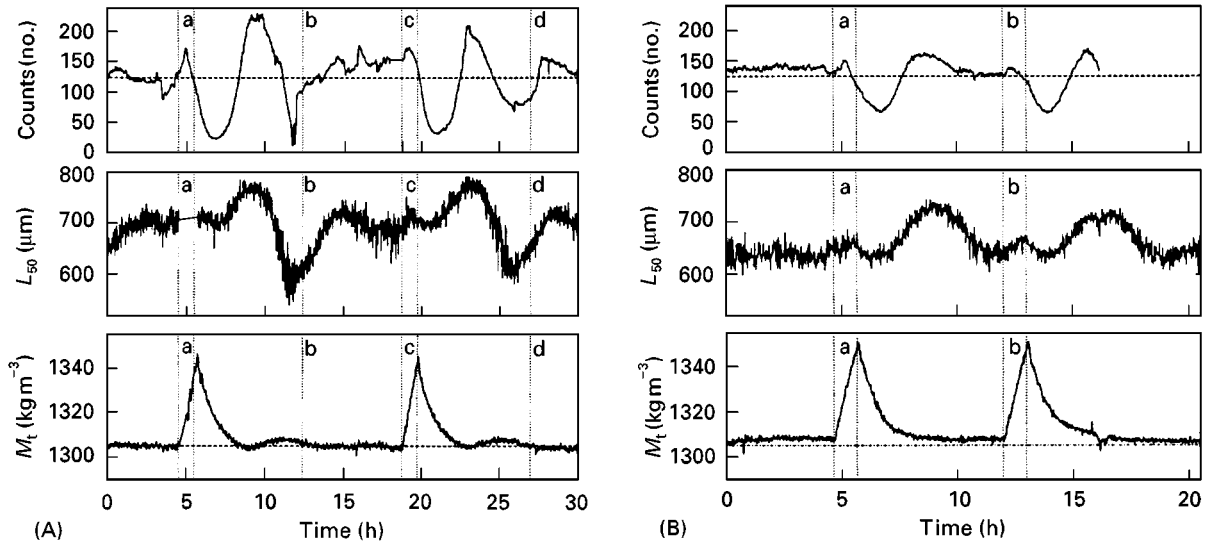

Figure 7 Measured (A) open and (B) closed loop responses of the counter signal, the median crystal size and the product magna density due to a disturbance in the product flow at a and c for the open loop experiment and at a and b for the closed loop experiment (Eek, 1995).

x is the vector of state variables. The crystallizer model must therefore be transformed into a state space representation. This can be achieved by the moment transformation, which is however only valid for a mixed suspension mixed product removal (MSMPR) type of crystallizer with simple crystallization kinetics. Application of the method of lines also yields a state space representation of the model.

An important topic in the design of a multivariable controller is the choice of the input–output pairs. On the basis of a relative gain array analysis with experiments done on a 1 m^3 KCl crystallizer, a control structure with the fines, the product and the feed flow rate as process inputs, and the mean crystal size, the weight percentage of solids and the supersaturation as process outputs has been proposed.

On the basis of a controllability analysis the median crystal size has been rejected as an output variable because of the long delays. The control structure shown in **Figure 8** was proposed as an alternative. This control structure was experimentally analysed on the 1000 L evaporative DTB crystallizer using a model predictive controller in combination with a state estimator. The controller was based on a linearized first principle model using the method of lines to transform the model into a state space representation. The controller showed good performance with respect to stabilization, disturbance rejection and setpoint tracking, which was slightly better than that of a multiloop PI controller. This improvement is related to the interaction, which is taken into account in a multivariable model predictive control (MPC) controller, and the better constraint handling of this controller.

Control of Batch Crystallizers

Batch crystallizers are used extensively for crystallization procedures that are of small capacity and have a high added value, and often when multipurpose reactors are used for the crystallization process. Therefore the control of a batch process differs considerably from that of a continuous process. In addition, although a batch crystallizer can be described by a similar model to the continuously operated crystallizer, because of the inherently nonstationary process conditions and the strong dominant role of the start-up phase on the product quality process conditions, a completely different control strategy must be followed.

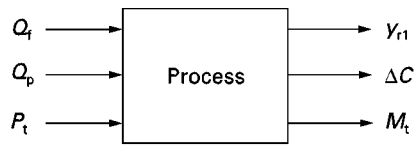

Figure 8 Input–output structure for a multivariable controller (Eek, 1995).

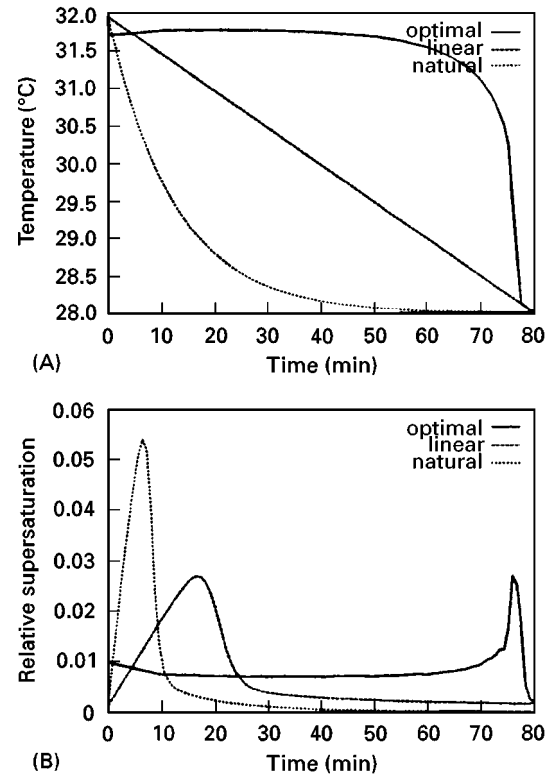

Figure 9 (A) Temperature profiles for a batch cooling KNO_3–H_2O crystallizer and (B) the resulting supersaturation in the crystallizer for different cooling policies (Miller and Rawlings, 1994).

Literature references to the control of batch crystallization processes are mainly directed towards finding cooling or supersaturation profiles (a supersaturation versus time trajectory) that optimizes the product quality of the crystals profile.

Cooling profiles have been determined directly from MSMPR crystallization models with some additional simplifications. Other studies use simulation to calculate a cooling profile that maintains a constant supersaturation or an optimal control theory in combination with an objective function for the final product. The problem with these studies is that they all are limited to strict crystallizer configuration (MSMPR, no fines removal), and simple kinetic models. In addition they are unable to incorporate constraints in the process variables.

An alternative approach is to solve the general multivariable optimal control problem as a nonlinear programming problem.

Using this approach an optimal cooling programme can be calculated. An example is shown in **Figure 9**, in which a natural, a linear and an optimal

cooling profile are given together with the resulting supersaturation profile for a KNO_3–H_2O system crystallized in a 3 L cooling crystallizer. The curves were determined using a first principle model in which four parameters were estimated using experimental data, maximizing the terminal seed size. Constraints were imposed on the crystallizer temperature and on the production yield. Experimental verification of the optimal cooling profile gave a 9% increase in the terminal seed size over that with linear cooling, and an 18% increase over that with natural cooling.

The determination of optimal cooling profiles is, however, not sufficient for an optimal operation of a batch crystallizer. Uncertainties in the start-up phase and in the crystallization model make the need for on-line measurements and a feedback control relevant. Depending on the reproducibility of the start-up phase, on line optimization procedures might be desirable for optimization of the process.

Conclusions

The control of both continuous and batch crystallizers has been shown to be feasible and can result in a considerable improvement of the process performance. Impressive results have been obtained even with a simple feedback controller, especially in the suppression of the process disturbances and in the stabilization of the process. This makes the application of this CSD control likely in industry in the near future. This progress is based on an extensive analysis of the crystallization process (including the derivation of a reliable process model), the available measurement techniques and the process actuators. On the other hand, because of limitations in the process actuators and the internal feedback loops in the crystallization process, variations in the product specifications (such as the median crystal size) were very limited, especially in continuous crystallization. The situation can only be improved by better crystallizer designs.

It has been shown that there are process models available, that can give a reasonable description of process behaviour. These models are however very empirical in nature and are in principle input–output models. They lack a fundamental description of the underlying (local) phenomena, which is needed to predict the influence of scale, geometry and the physical/chemical properties of the crystallization system. Only then we will be able to design crystallizers and control systems without the need for an extensive research programme.

A better understanding and description of the local crystallization phenomena may also be the key for the improvement of the multivariable controllers by a better description of the interactions. Results have shown that there is no incentive for a multivariable controller, because the simple feedback controller gives comparable results with much less effort.

Symbols Used

b, g, h, j	Kinetic parameters
B_0	Birth rate (no. $m^{-3} s^{-1}$)
$B(L)$	Birth rate (size based) (no. $m^{-3} m^{-1} s^{-1}$)
C	Concentration (kg m^{-3})
C_p	Specific heat (J $kg^{-1} K^{-1}$)
C_s	saturation concentration (kg m^{-3})
$D(L, t)$	Death rate (no. $m^{-3} m^{-1} s^{-1}$)
G_L or G	Linear growth rate (m s^{-1})
H	Enthalpy
H_{cr}	crystallization enthalpy (J kg^{-1})
$h(L)$	Classification function (–)
K_N	Nucleation rate constant (–)
k_{distr}	Distribution constant impurity uptake (–)
k_g	Growth rate constant (m s^{-1})
L	Particle length [m]
m_j	jth moment of a distribution (–)
M_T	Total crystal mass per unit crystallizer volume (kg m^{-3})
N_{comp}	No of components (–)
$n(L)$	Number density (no. $m^{-3} m^{-1}$)
P	Production rate (kg s^{-1})
p1 … p9	kinetic parameters
t	time (s)
u	process input
V	Crystallizer volume (m^3)
y	process output
y_r	control signal derived from measured light diffraction pattern of the product crystals
w	Mass fraction (–)
ϕ_v	Volumetric flow rates ($m^3 s^{-1}$)
ε	Fraction free liquor (–)
ρ	Material density (kg m^{-3})
σ	Relative supersaturation (–)
τ	Residence time (s)

Further Reading

Beckman JR and Randolph AD (1977) Crystal size distribution dynamics in a classified crystalliser: part II, simulated control of crystal size distribution. *American Institute of Chemical Engineers Journal* 23: 510–520.

Eek RA, Pouw HAA and Bosgra OH (1995) Design and experimental evaluation of stabilising feedback controllers for continuous crystallisers. *Powder Technology* 82(1): 21–35.

DropBooks

Eek RA, Dijkstra SJ and van Rosmalen GM (1995b) Dynamic modelling of suspension crystallizers, using experimental data. *American Institute of Chemical Engineers Journal* 41(3): 571–584.

Kramer HJM, Bermingham SK and van Rosmalen GM (1999) Design of industrial crystallisers for a required product quality. *Journal of Crystal Growth* 198/199: 729–737.

Miller SM and Rawlings JB (1994) Model identification and control strategies for catch cooling crystallisers. *American Institute of Chemical Engineers Journal* 40: 1312–1327.

Ó Meadhra RS, Kramer HJM and van Rosmalen GM (1995) A model for secondary nucleation in a suspension crystallizer. *American Institute of Chemical Engineers Journal* 42(4): 973–982.

Randolph AD and Larson MA (1988) *Theory of Particulate Processes*, 2nd edn. New York, Academic Press.

Randolph AD, Chen L and Tavana A (1987) A feedback control of CSD in a KCl crystallisation with fines dissolver. *American Institute of Chemical Engineers Journal* 33: 582–591.

Randolph AD, Beckman JR and Kralievich ZI (1977) Crystal size distribution dynamics in a classified crystalliser: part 1, experimental and theoretical study of cycling in a potassium chloride crystallisation. *American Institute of Chemical Engineers Journal* 23: 500–510.

Rawlings JB, Miller SM and Witkowski WR (1993) Model identification and control of solution crystallisation processes. *Industrial and Engineering Chemistry Research* 32: 1275–1296.

Rawlings JB, Sink CW and Miller SM (1995) Control of crystallisation processes. In: Meyerson A (ed.) *Handbook of Industrial Crystallisation*, pp. 103–130. Boston: Butterworth Heinemann.

Redman T, Rohani S and Strathdee G (1997) Control of the crystal mean size in a pilot plant potash crystalliser. *Transactions of the Institute of Chemical Engineers* 75A: 183–192.

Rohani S (1995) Control of crystallisers. In: Mersmann A (ed.), *Crystallisation Technology Handbook*. New York: Marcel Dekker, Inc.

Dynamic Behaviour

See **II / CRYSTALLIZATION / Control of Crystallizers and Dynamic Behaviour**

Geocrystallization

J. A. Gamble, School of Earth Sciences, Victoria University of Wellington, New Zealand

Copyright © 2000 Academic Press

Magmas are hot (eruption temperatures range between 600°C and 1400°C), multicomponent, but generally silicate-dominated melt systems formed by processes of partial melting in the interior of the earth. Silicon and oxygen are the major constituents of most magmatic systems, apart from those of the carbonatite association, where $NaCO_3$ and $CaCO_3$ are significant components. This article considers crystallization in silicate-dominated melt systems. In addition to Si and O, Ti, Al, Fe^{3+}, Fe^{2+}, Mn, Mg, Ca, Na, K and P comprise the constituents commonly referred to as the 'major elements'. It has become conventional to refer to these in terms of their oxides, expressed in weight percent (**Table 1**). Furthermore, magmas typically contain dissolved volatile species, dominated by H_2O, but including SO_2, H_2S, Cl_2, F_2, CO_2, CO and traces of noble gases such as He, Ar and Xe. Elements such as Rb, Sr, Ba, Zr, Nb, the rare earth elements, Pb, Th and U are present in trace amounts (typically μg g^{-1} or ppm) and are called 'trace elements'.

After magmas form, they may move away and separate from their source regions, due principally to

Table 1 Major oxide chemical analyses (wt%) of typical volcanic igneous rocks. All data are from the author's database of chemical analyses

Element oxide	*Basalt*	*Andesite*	*Dacite*	*Rhyolite*
SiO_2	49.86	60.35	66.68	73.89
TiO_2	1.38	0.78	0.58	0.33
Al_2O_3	15.96	17.53	16.5	13.69
Fe_2O_3	5.47	3.37	2.42	1.47
FeO	6.47	3.17	1.93	0.89
MnO	0.32	0.18	0.06	0.08
MgO	6.27	2.79	1.43	0.39
CaO	9.1	5.87	3.51	1.22
Na_2O	3.16	3.63	4.03	3.43
K_2O	1.55	2.07	2.71	4.53
P_2O_5	0.46	0.26	0.15	0.08